AD-A048 803 ROCKWELL INTERNATIONAL ANAHEIM CA ELECTRONIC DEVICES DIV F/G 9/5
AN ELECTRICAL SURGE ARRESTOR (ESA) MODEL FOR COMPUTER-AIDED DES--ETC(U)
NOV 77 C T KLEINER
UNCLASSIFIED X77-1102/501 NL

| OF |
AD
A048803

END
DATE FILMED
2-78
DDC

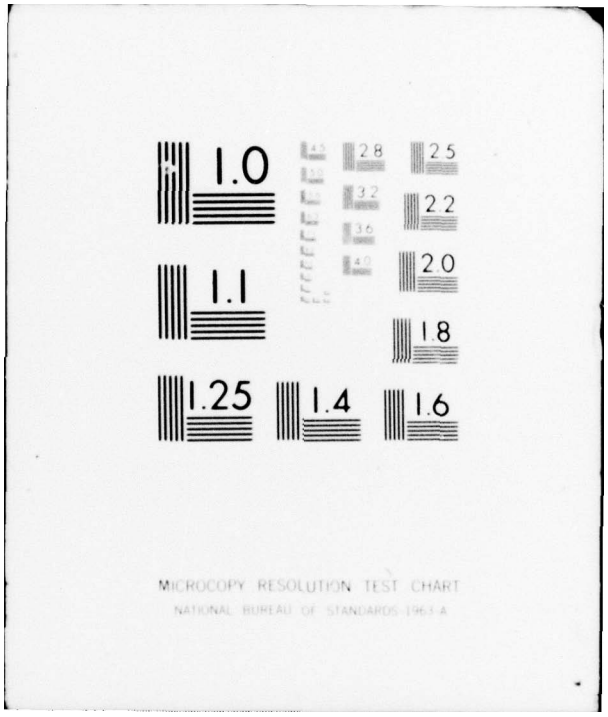
1.0
1.1
1.25
1.4
1.6
2.8
2.5
3.2
2.2
3.6
2.0
4.0
1.8
MICROCOPY RESOLUTION TEST CHART
NATIONAL BUREAU OF STANDARDS-1963-A

AD A048803

technical information from ...

Rockwell International

(1)

(6) AN ELECTRICAL SURGE ARRESTOR (ESA) MODEL FOR COMPUTER-AIDED DESIGN AND EVALUATION

(11) 2 November 1977

(12) 8p.

By

(10) C. T. Kleiner

(21) ~~Presented to:~~ Presented at the ~~Eleventh~~ Annual Asilomar Conference on Circuits, Systems and Computers (11th).

(14) X77-1102/501

THE DISTRIBUTION OF THIS REPORT IS UNLIMITED

Rockwell International

Electronics Research Center
Electronic Devices Division

3370 Miraloma Avenue
P.O. Box 4182
Anaheim, California 92803

AN ELECTRICAL SURGE ARRESTOR (ESA) MODEL FOR COMPUTER-AIDED DESIGN AND EVALUATION

AN ELECTRICAL SURGE ARRESTOR (ESA) MODEL FOR COMPUTER-AIDED DESIGN AND EVALUATION

by

C. T. Kleiner
Rockwell International Electronic Devices Division
Anaheim, California

I. Summary

Electrical Surge Arrestors (ESA's) are widely used to protect susceptible electrical and electronic components sub-systems and systems from the potentially damaging effects of lightning, static discharge, Electromagnetic interference and the Electromagnetic pulse arising from potential nuclear weapon detonations. ESA's are very non-linear devices when operating near or above the DC breakdown potential. The ESA model to be described accounts for a significant number of nonlinear effects including (1) streamer formation, (2) plasma conductivity, (3) glow region, (4) arc extinguishing, (5) high frequency oscillations, (6) Thermionic effects, and (7) heating and heat dissipation to the surrounding medium. The model is illustrated in Figure 1 with a corresponding definition for each parameter in the model.

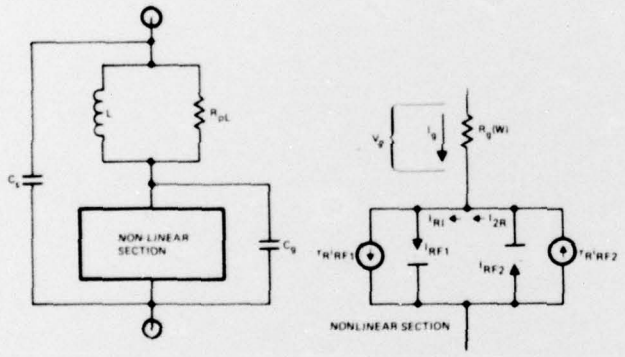

Figure 1. Electrical Surge Arrestor (ESA) Model

II. Model Parameters and Equations

Figure 1 illustrates the equivalent circuit for the Electrical Surge Arrestor model. The linear portion of the model is defined by the L, R_{pL}, C_g and C_s elements. The nonlinear portion of the model is also illustrated and basically represents the complex reaction of initial streamer/arc formation followed by plasma formation and includes the Thermionic potential observed during the ON or conduction phase of ESA operation. The various model parameters, nonlinear equations which utilize the parameters will be defined and illustrated by model application and comparison to test results. The various test circuits are also shown for the benefit of other investigators wishing to characterize ESA's or spark gaps in a manner described herein.

Definition of Model Parameters and Equations

1. Linear Section

L = Lead Inductance (usually in nano henries)

R_{pL} = Flux loss ("Q") associated with L (usually in K ohms)

C_S = Stray Capacitance (reflected capacitance at the ESA terminals from all other sources, leads, etc.)

C_f = Gap Capacitance (measured or calculated for the Gap)

2. Nonlinear Section

(a) R_g = A nonlinear resistor dependent on the energy being dissipated within the gap and transferred to the surrounding medium

Equations:

$$R_g = \frac{K_1}{W} \tag{1}$$

$$W = W_{IN} - W_{OUT} \tag{2}$$

$$W_{IN} = \int \left[\frac{V_g^2}{R_{gn-1}} \right] dt \tag{3}$$

$$W_{OUT} = \int \frac{W}{\tau_d} dt \text{ or } \int P_{ml} dt; \tag{4}$$

(whichever is less)

where:

R_g = Instantaneous Resistance of the gap (ohm)

V_g = Instantaneous Voltage across the gap (volts)

I_g = Instantaneous Current through the gap (amps)

W = Instantaneous Energy in the gap (joules)

W_{IN} = Instantaneous Energy generated as input to the gap (joules)

W_{OUT} = Instantaneous Energy removed from the gap to the surrounding medium (joules)

K_1 = Scale factor relating R_g to W (Ω-joules)

P_{m1} = Maximum instantaneous power lost to the surrounding medium (watts)

τ_d = Dissipation time constant (an average thermal time constant for establishing the rate at which heat energy (joules) is dissipated to the surrounding medium) (sec)

R_{gmax} = Maximum resistance of the air gap (ohms)

R_{gmin} = Minimum resistance of the air gap (ohms)

W_{min} = Minimum energy in the air gap (joules)

V_{DB} = Gap breakdown threshold voltage (volts) $V_{DB} \approx 100$KV/inch in air at STP

τ_{SF} = Time for Streamer Formation (τ_{SF} increases with gap width)

I_{gmin} = Instantaneous value of arc current below which the arc extinguishes.

The following controls are employed:

No. 1 If $V_g \geq V_{DC}$ and $W \geq 0$, then initiate timer at t_o (time at which the condition for streamer formation has been achieved)

No. 2 At $t = t_o + \tau_{SF}$ initiate computation of W and subsequent modification of R_g (see Figure 2 characteristic curve)

No. 3 Continue to monitor W until $W \leq W_{min}$. Also monitor R_g and limit R_g to R_{gmin} by comparing $R_g(W)$ to R_{gmin}

No. 4 Return R_g to R_{gmax} when gap is fully extinguished $I_g \leq I_{gmin}$

(b) Thermionic Effect = The phenomenon that accounts for the high ON voltages observed in ESA's (over 100 volts), whereby the emitting ESA block effectively becomes a cold cathode, while the collecting ESA block becomes the plate, in what is essentially Thermionic reaction, namely, the plasma creates a junction which is represented mathematically by the following equations:

$$I_{RF1} = I_{S1} (\exp VR/M_1\theta) - 1) \quad (5)$$

$$I_{RF2} = I_{S2} (\exp -VR/M_2\theta) - 1) \quad (6)$$

where:

V_R = Thermionic junction potential (volts)

I_{S1}, I_{S2} = A pseudo-saturation current for the Thermionic Rectifier (and are also functions of temperature and effective plasma area)

M_1, M_2 = Multiplier for empirical fit (M has a range of 50 to 500 depending on the particular ESA) (non-dimensional)

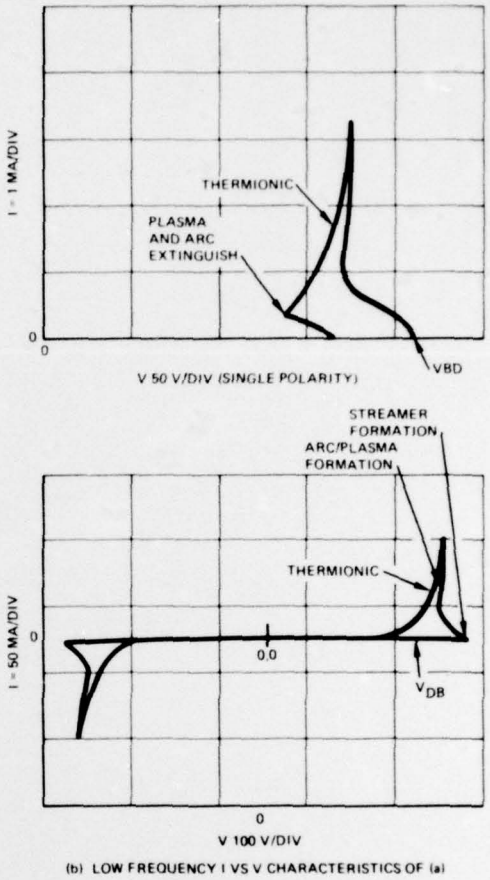

Figure 2. Non-Linear Section of ESA Model and Low Frequency I (V) Characteristics

In addition, there is a slight tendency for these "Thermionic Rectifiers" to "store" charge similar to a semiconductor rectifier, hence, the net current in each Thermionic Rectifier is formulated as follows:

$$I_{R1} = I_{RF1} + \tau_R \dot{I}_{RF1} \quad (7)$$

$$I_{R2} = I_{RF2} + \tau_R \dot{I}_{RF2} \quad (8)$$

where:

τ_R = Thermionic electron recombination time (which is believed to be on the order of a few nanoseconds)

$$\theta = kT/q = .026 \text{ @ } 27^{\circ}C \quad (T \text{ is set @ } 300^{\circ}K) \quad (9)$$

A set of typical ESA model data is shown in Table I.

Using non-linear model shown in Figure 1, and the data shown in Table I, it was possible to analytically obtain I versus V characteristics showing the extremely non-linear behavior of the gap for (1) Streamer, (2) Arc/plasma, and (3) Thermionic formation including extinguishing of the arc. This is shown in Figure 2.

Table I. Example of ESA Data

	Parameter	Value	Units
Linear Section	L	130	nh
	R_{pL}	2500	ohms
	C_g	3.18	pfd
	C_s	1	pfd
Nonlinear Section Rg	K_1	$2^{/-3}$	ohm-Joules
	P_{m1}	1500	Watts
	τ_d	.1	usec
	R_{gmax}	$1^{/+12}$	ohms
	R_{gmin}	.1	ohms
	W_{min}	$1^{/-10}$	Joules
	V_{DB}	185	Volts
	τ_{SF}	1	nsec
	I_{gmin}	5	ma
Thermionic	I_s	1	ua
	M	500	-
	τ_R	.1	nsec

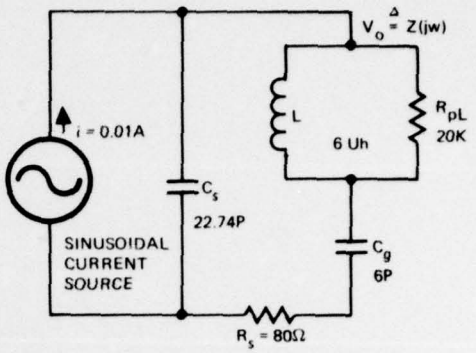

(a) SMALL SIGNAL EQUIVALENT CIRCUIT (FIGURE 1 LINEAR SECTION)

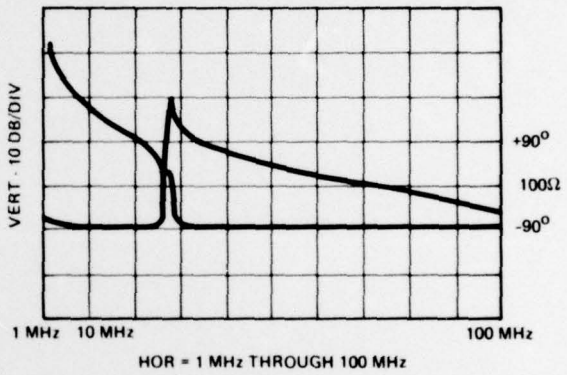

(b) LABORATORY TEST RESULTS (USING HP NETWORK ANALYSER)

Figure 3. Small Signal Equivalent Circuit for Audio ESA (Below Breakdown) and Laboratory Test Response

III. ESA CHARACTERIZATION

Several types of ESA's were modeled and characterized (Audio, Power and Antenna ESA's) for both the linear and non-linear components of the model.

The linear characteristics can be obtained quite readily by using a network analyzer and solving for the values of L, C_S, C_g, and R_{pL}. The result for an Audio ESA is shown in Figure 3.

The nonlinear characteristics are considerably more difficult to obtain.

The following tests were conducted to obtain the nonlinear characteristics:

1. Sawtooth Oscillator Test

The first test that can be performed is shown in Figure 4 where the ESA is used as the nonlinear element which produces a sawtooth oscillation. Resistor, R_1, must be sufficiently large so that the 'holding current' will not sustain a very low electron leakage and prevent oscillation. This determines one of the critical parameters, namely, the minimum power to sustain the arc. This may not be the minimum power required to completely describe the interaction of the plasma with the surrounding medium however. The dynamic resistance of the arc can appear quite high even though the capacitor, C_1 is a very low impedance source at the switch point and hence, would be expected to discharge rapidly giving rise to a high current pulse through the ESA; this is not the case for this or other ESA's. The reason for this apparent high discharge impedance in this sawtooth oscillator configuration is postulated to be due to the relatively high resistance of R_{gap} and the relatively high impedance of the onset of the Thermionic conduction

$$\frac{M_\theta}{I_{gap}}$$

2. Fast Rise Time Test

When the ESA is subject to a high voltage, fast rise-time input, two characteristics become apparent. First, the firing potential increases and second, the ON voltage is only somewhat higher than during the sawtooth operation. The dynamic resistance becomes much lower which satisfies the functional relationship between R_{gap} and M_θ/I_{gap} (both resistors being inverse to arc current density). The high dv/dt input results in a voltage breakdown vs rise-time characteristics as shown in Figure 5. There are two regions of the curve which are worthy of discussion. Region I shows a fairly gradual increase in apparent gap breakdown with increasing dv/dt. This increase is attributable to the interaction of the arc formation and energy dissipation coupled with the effect of the reactive linear elements (L's and C's) of the ESA. In Region II the apparent breakdown of the ESA vs dv/dt increased more rapidly. This is attributed to the time required for streamer formation. This occurs prior to arc formation. The net effect of this ESA response to very high values of dv/dt (or high frequency) reduces ESA effectiveness for the high frequency components of disturbance.

0.2 SEC/DIV
(a) TEST RESPONSE (VOLTAGE)

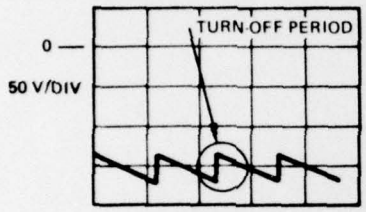

0.2 SEC/DIV
(b) COMPUTER SIMULATION (VOLTAGE)

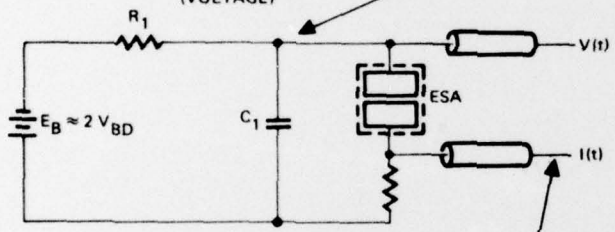

(c) SAWTOOTH TEST CIRCUIT

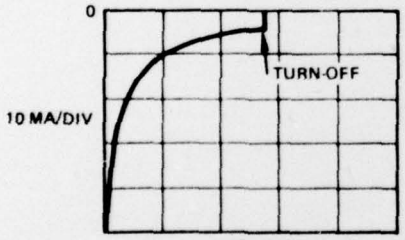

1 MSEC/DIV
(d) COMPUTER SIMULATION (CURRENT) (TURN-OFF PERIOD)

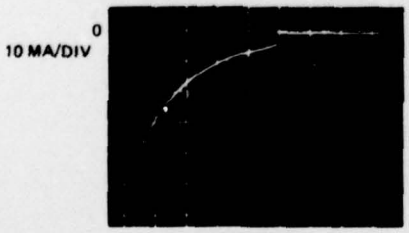

0.5 MSEC/DIV
(e) TEST RESPONSE (CURRENT) (TURN-OFF PERIOD)

Figure 4. Sawtooth Oscillator Test Results and Comparison to Computer Model Response

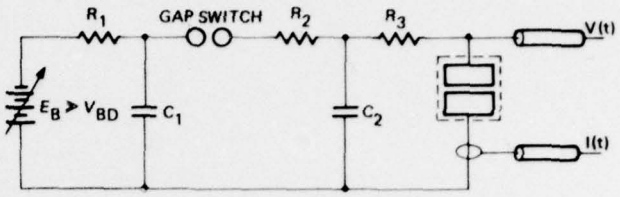

(a) FAST RISE TIME TEST CIRCUIT (R_1 = 1 MEG, C_1 = 0.02 UFD, $R_2 = R_3 = 510\Omega$, C_2 VARIED FROM 50 PFD THROUGH 350 PFD)

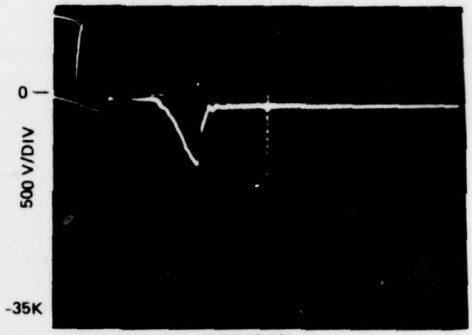

100 NSEC/DIV
(b) REST RESULTS (VOLTAGE)

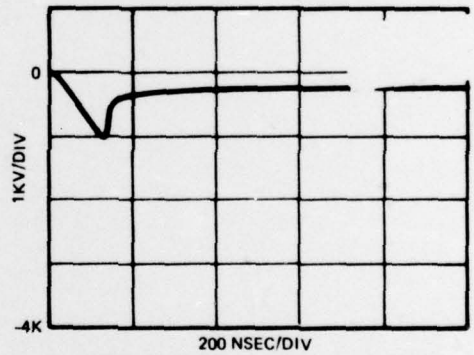

200 NSEC/DIV
(c) COMPUTER MODEL RESPONSE (VOLTAGE)

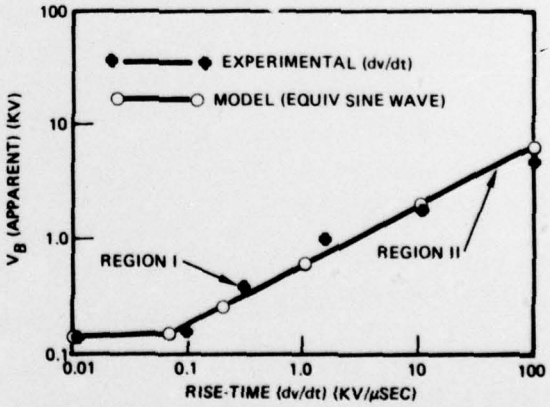

(d) PLOT OF INCREASED BREAKDOWN VOLTAGE V_B (APPARENT) VS RISE TIME (dv/dt) OR EQUIVALENT FREQUENCY f

Figure 5. Characterization of Increase in Apparent Voltage Breakdown (or Overshoot) vs Rise Time Test Circuit, Results and Plot of V_B vs dv/dt

3. Damped Sine Wave Test

In practice a damped sinewave is frequently used to characterize component and/or subsystem response to Electrical Surges. As a result, the ESA and corresponding model were also characterized using various damped sinewave input stimulus. The result of this test and model simulation as illustrated in Figure 6. Note that the ESA's can open after the initial shorting if the sustaining energy is insufficient to cause the arc to sustain. This is particularly true for lower frequencies (~1 MHz and below) and higher impedance (>1 KΩ) sources.

IV. Example Computer Coding for the ESA Models Using SYSCAP II

The SYSCAP II program was used to perform several studies involving the spark gaps and surge arrestors discussed in Section III. This section will illustrate how some of these models were programmed using the SYSCAP II ALCAP and TRACAP subprograms.

ALCAP: The ALCAP (A. C. Linear Computer Analysis Program) was used to model the linear network shown in Figure 3. Figure 7 illustrates the coding list used to obtain the results shown in Figure 3. In addition to the amplitude and phase vs frequency response, the ALCAP program was also used to determine the sensitivity of the amplitude and phase response to component tolerance at various frequencies. This capability of the program was very useful in characterizing the networks since it identified which elements were the most critical. It showed that L and C_g were very critical around resonance while R_{pL} and C_s were not as sensitive.

TRACAP: The TRACAP (TRAnsient Computer Analysis Program) was used to model the combined linear and non-linear model shown in Figure 1. Figure 8 illustrates an example of TRACAP coding used to obtain the non-linear I(v) characteristics (as shown in Figure 2). It should be noted that there is a significant negative resistance region which is characteristic of spark gaps which has been very difficult to model in the past but posed no significant problems using the TRACAP code due to the conservative convergence algorithms that have been used.

Another example of TRACAP application for ESA modeling is illustrated in Figure 9 where a damped sinewave stimulus simulates a potential surge disturbance. The results are compared to test data shown in Figure 10. In this case two functions are used, namely FUNC 1 to characterize the ESA resistance $R_g(W)$ and FUNC 2 to generate the exponentially damped sine wave:

$$f_2 = A\epsilon^{-(t/t)} \sin(wt).$$

These examples have been given so that scientists and engineers who are interested in this type of model (surge protection analysis/design) can readily avail themselves of this capability via the SYSCAP program.

V. Conclusions

The ESA model presented in this paper is relatively easy to use (in an appropriate computer program such as SYSCAP II) and permits a detailed evaluation spark gap protection to a variety of electrical surge stimulus. The model accounts for the extremely nonlinear behavior of the ESA gap including intermittent firing, variation in ON impedance and other related phenomenon. Examples of model application demonstrate the behavior of the model in the linear and non-linear regions.

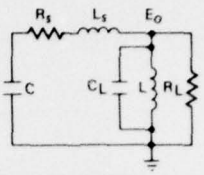

(a) EQUIVALENT CIRCUIT FOR DAMPED SINEWAVE PULSER (R_S INCLUDES NONLINEAR GAP RESISTANCE)

(b) LAB TEST RESULTS
VERT = 300 V/DIV
HOR = 100 NS/DIV

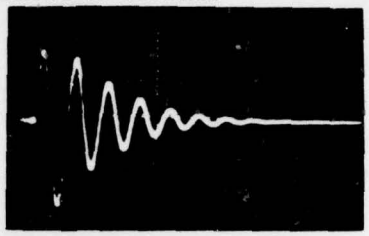

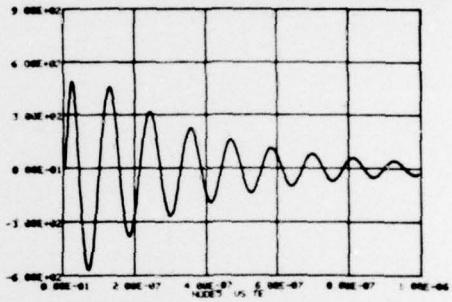

EXAMPLE OF PULSER MODEL (C/R) USING SIMPLE EQUIVALENT CIRCUIT LAB TEST RESULTS

(c) EQUIV CIRCUIT RESPONSE (PDP8e) VERT = 300 V/DIV
HOR = 200 NS/DIV

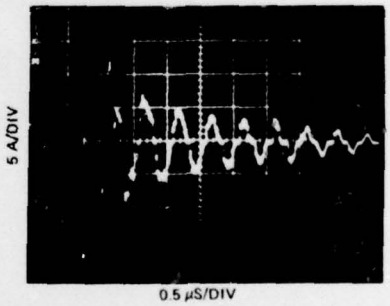

(d) LAB TEST RESPONSE USING DAMPED SINE WAVE PULSER

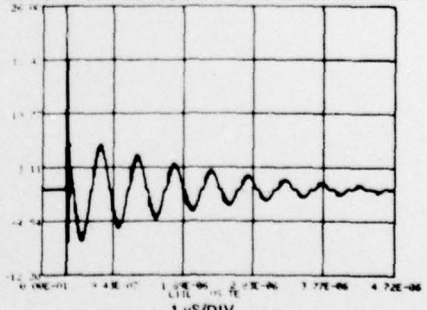

(e) ESA MODEL RESPONSE (INCLUDING SHORT INDUCTANCE LOOP RINGING) (TEKTRONIX 4010)

Figure 6. Comparison of ESA Lab Tests (Damped Sinewave) and ESA Model Response (Tektronix 4010 Display)

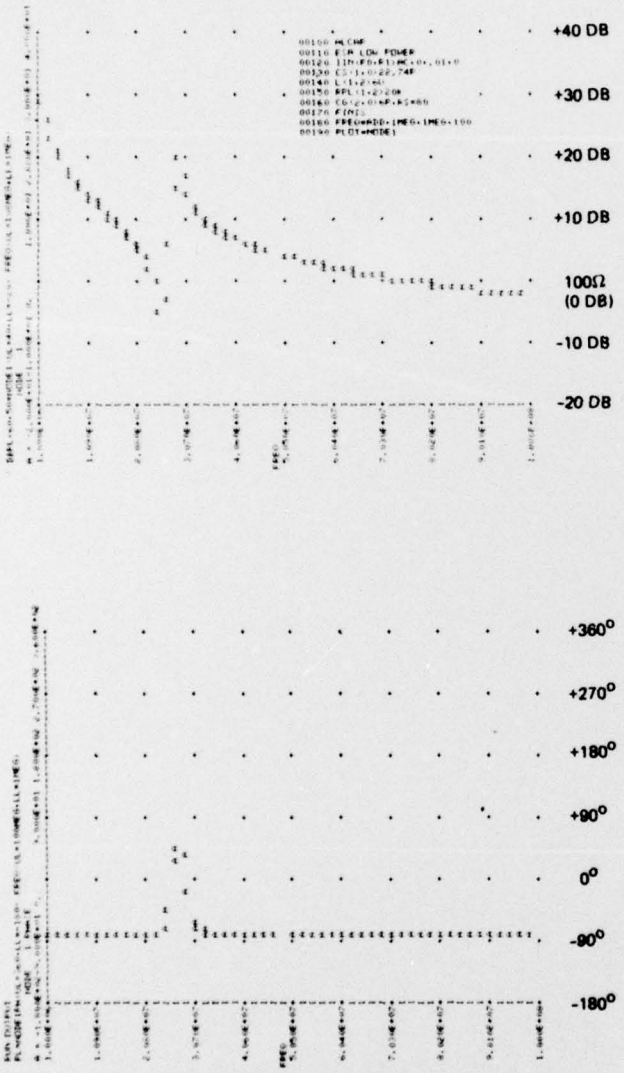

Figure 7. SYSCAP II (ALCAP) Coding and Amplitude/Phase Response Using a TI Silent 700 Terminal

(a) CODING

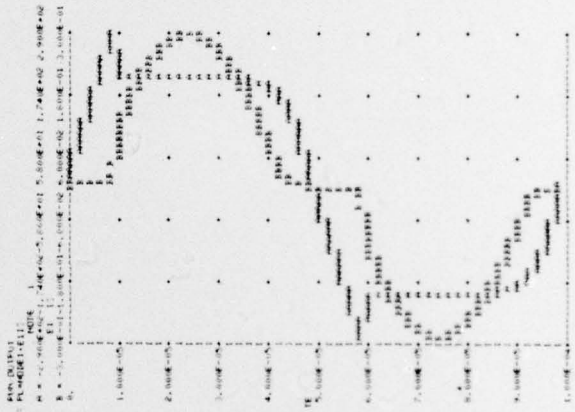

(b) VOLTAGE (A) AND CURRENT (B) VS TIME (TI SILENT 700)

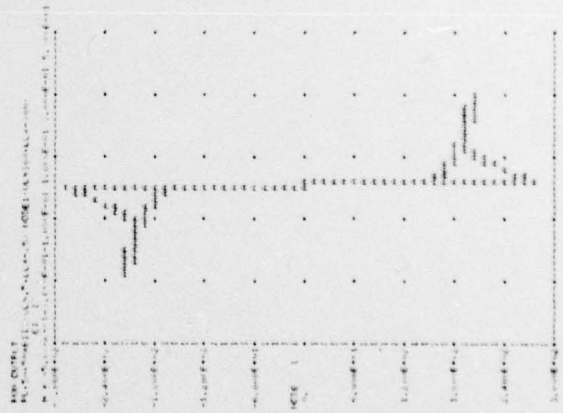

(c) PLOT OF I VS V (NODE 1)

Figure 8. Illustration of Interactive SYSCAP II (TRACAP) Coding and Response Using a TI 700 Terminal

VI. References

1. SYSCAP II User Information Manual (Publication No. 76070600), Available through CDC Cybernet Data Services Publications, P.O. Box O, HQW05F, Minneapolis, MN 55440

(a) CODING

(b) PLOT OF NODE 1, 2,
CURRENT (E1IS) THROUGH
ESA AND GAP RESISTANCE

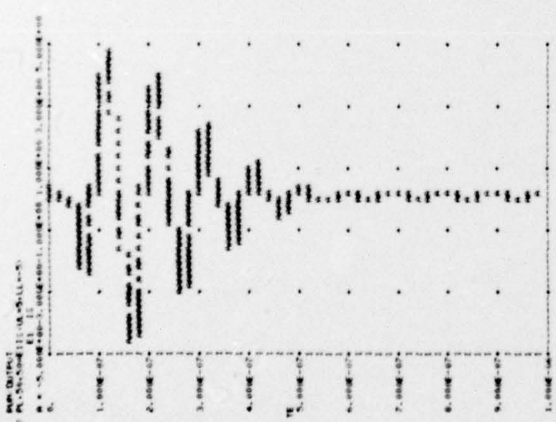

(c) CURRENT VS TIME

Figure 9. Illustration of Interactive SYSCAP II (TRACAP) Coding and Response for a Damped Sinewave Input

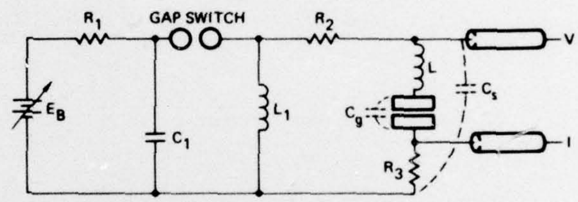

(a) DAMPED COSINE TEST CIRCUIT $[R_1 \gg R_2, R_2 = R_3 = 50\Omega,$ $f_o = 1/2\pi\sqrt{L_1C_1}, Q \geq 7 = 2\pi f_o L_1/(R_2 + R_3)]$

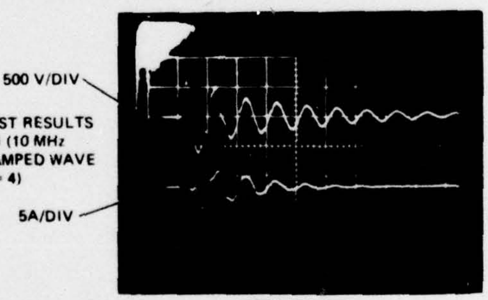

(b) TEST RESULTS f(t) (10 MHz DAMPED WAVE Q = 4)

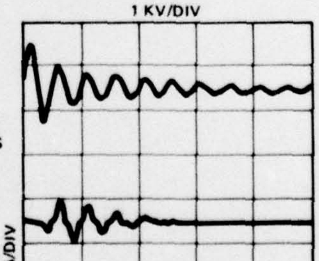

(c) MODEL RESPONSE (INCLUDES RINGING DUE TO L, $C_g + C_s$)

Figure 10. Test Circuit and Response Comparison for a Damped Sinewave